

INVESTIGATION INTO THE EFFECTIVENESS OF ADVANCED DRIVER AIRBAG MODULES DESIGNED FOR OOP INJURY MITIGATION

Jörg Hoffmann

Michael Freisinger

Toyoda Gosei Europe N.V.

Germany

Mike Blundell

Manoj Mahangare

Faculty of Engineering and Computing, Coventry University

United Kingdom

Peter Ritmeijer

TNO Automotive Safety Solutions

Netherlands

Paper Number 07-0319

ABSTRACT

In accordance with National Highway Traffic Safety Administration (NHTSA) regulations and, in particular the Federal Motor Vehicle Safety Standard (FMVSS) 208 for the protection of vehicle occupants from a deploying airbag, the development of frontal restraint systems is driven by new technologies and technical solutions to cover the challenging out-of-position (OoP) load case. Considering the subject of the driver airbags, traditional module technology addressed only the energy absorption capability to protect the driver occupant while in-position for a severe frontal crash load case. The early unfolding characteristics of the deploying airbag and its physical effects on the environment did not therefore form part of the engineering focus at that time. This paper will discuss an advanced driver airbag (DAB) module devised to deploy in an initially less aggressive mode, thereby exposing occupants seated OoP and close to the airbag's effective working area to less risk. The airbag inflation is divided into a primary and a secondary deployment phase by chambering the cushion with internal gas deflection fabric walls. After reaching an internal threshold pressure, these walls fail at a predetermined energated split line. This leads to full bag deployment to ensure full energy absorption potential for the occupant seated in-position during the crash loading. This sophisticated deployment characteristic is simulated using a numerical approach to represent the actual fluid flow within the airbag to reproduce the airbag's initial unfolding process. Initial simulations

recreate a simple physical (pendulum) laboratory test scenario. Further consideration of the OoP performance of the advanced airbag module is provided by replacing the simple pendulum with the more complex digital female frontal dummy positioned in accordance with the FMVSS 208 standard. Finally, the results obtained using the advanced airbag occupant simulation methodology are compared with the results of OoP occupant tests.

Keywords: Airbag, OoP, MADYMO, CFD, Gasflow

INTRODUCTION

Studies indicate that airbags have reduced deaths in frontal crashes by about 26 per cent for belted drivers and by about 32 per cent for unbelted drivers [1]. Fatalities in frontal crashes have also been further reduced by 14 per cent for belted and by 23 per cent for unbelted passengers [2]. The National Highway Safety Administration (NHTSA) estimates that as of May 1998, airbags had saved nearly 3 000 lives in the United States [3]. Thus, airbags are effective in reducing the risk of death and injury associated with many severe frontal car crashes.

Despite overall effectiveness, real-world experience has shown that some unbelted (OoP) occupants are being injured and even killed by deploying airbags. As of May 1998, NHTSA attributed 99 deaths in low-severity crashes to airbag inflation energy. These deaths include 38 adult drivers, 4 adult passengers (a

belted 98-year-old female and an unbelted 88-year-old female, an unbelted 57-year-old male and an unbelted 66-year-old female, 44 children aged 1-11 and 13 infants (10 restrained in rear-facing infant seats and 3 seated on adult passenger laps). In response to these side-effects of an airbag in low- and moderate-severity crashes, FMVSS 208 issued by NHTSA in May 2000, proposed that static OoP tests should be a mandatory requirement starting in 2003 [4]. These tests include performance requirements to ensure that airbags developed in the future do not pose an unreasonable risk of serious injury to OoP occupants. For the driver side, there are two static OoP test positions using a 5th percentile female dummy as illustrated in the following Figure 1.

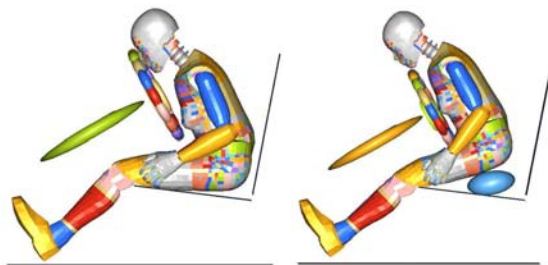


Figure 1. Dummy posture for driver-side OoP test according to FMVSS 208

To achieve occupant protection during a crash using a fully-deployed airbag to dissipate the frontal crash forces experienced by the driver over a larger body area and gradually decelerate the occupant's head and torso to prevent contact with other interior surfaces, the airbag itself must deploy rapidly in less than 50 milliseconds. Consequently, an occupant positioned extremely close to the airbag module at the time the airbag begins to inflate is exposed to highly localised forces [5]. Two phases of airbag deployment have been associated with high, injury-causing localised forces: the punch-out phase and the membrane-loading phase [6]. The punch-out phase occurs before or immediately after an airbag escapes from the module. If this escape is blocked by an unconscious driver slumped over the steering wheel, the resulting high force is concentrated on that part of the driver blocking the airbag's deployment path. The membrane-loading phase occurs after the airbag is out of the module. The injury-causing forces during this phase result from a combination of the airbag's internal pressure and the tension forces arising from the inflating airbag wrapping around the occupant.

To address the low risk deployment requirement of the FMVSS208 standard, the following parameters, which influence the functional design process of restraint systems, should be considered:

- Inflator (dual-stage, mass flow characteristic, diffusers, gas outlets, power) [7],
- Cushion geometry (chambered, vents, straps, mounting) [8],
- Folding pattern [9],
- Airbag door opening (tear seam geometry, material) [10].

To cover the FMVSS208 occupant OoP load case on the driver's side, Toyota Gosei has developed an advanced airbag design that features a cushion geometry which is initially separated into two chambers by internal tethers. Targeting a less aggressive primary deployment (punch-out phase) as well as a less aggressive radial secondary deployment (membrane-loading phase), the following Figure 2 explains the deployment characteristics of the advanced cushion compared to a conventional cushion.

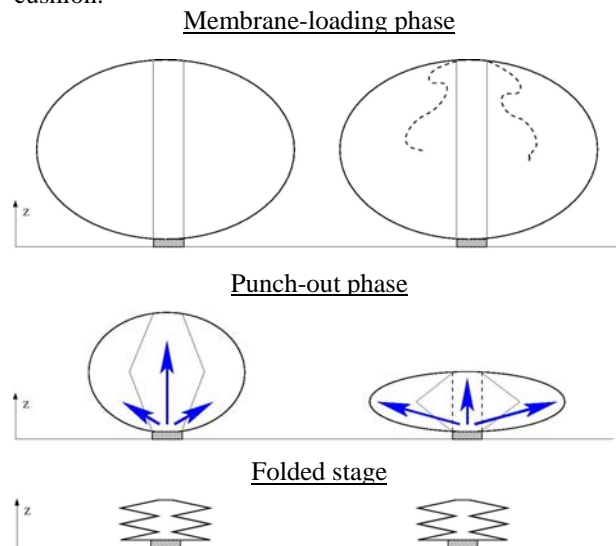


Figure 2. Deployment phases of a conventional airbag design (left) versus the advanced airbag design (right)

On the left, the deployment kinematics of a conventional DAB are shown to be directed mainly towards the occupant. By contrast, the advanced airbag deploys more laterally in the plane parallel to the occupant's head (right). If the internal pressure increases to a certain threshold, the internal chamber walls will rupture. This leads to the full deployment that would be needed to cover the kinetic energy absorption at in-position load cases including the conventional tethers. Because at the same time local low risk deployment and global restraint performance must be guaranteed, the design of the advanced airbag must meet the conflicting objectives of keeping the released energy as low as possible, while

at the same time maintaining acceptable crash protection performance.

The only plausible solution to master this challenge makes use of CAE simulation processes which help to find an optimised compromise between risk and protection as discussed in [11]. For frontal restraint systems, occupant protection CAE methods based on Finite Element Modeling (FEM) and Multi-Body-System (MBS) have evolved into powerful tools with a high degree of maturity. Unlike protection situations where interaction between the airbag and the occupant does not occur until the airbag is fully deployed, in risk situations, the occupant interacts with the airbag at an early stage of deployment. Typical characteristics of an OoP airbag simulation model, which covers the early inflation of a folded airbag, are listed in accordance with [12] as follows:

- highly unsteady phenomenon,
- wide range of gas flow speeds (supersonic to transonic),
- coupled moving boundaries of the airbag interact with gas flow and deform in space and time,
- unfolding of a folded airbag (contact characteristics).

Safety system engineers studied the inflation process of fully folded airbags based on uniform pressure (UP) distribution within the airbag volume [13] at quite an early stage. The implementation of real gas flow computer fluid dynamics (CFD) approaches, combined with improved contact algorithms in the safety system simulation tools Ls-Dyna, Pam-Crash and Madymo, that are commonly used in the industry, was mainly driven by the FMVSS 208 standard issued by NHTSA in 2000 (please refer to [14], [15], [16], [17] and [18]).

As a world-wide standard in restraint system simulation, the study accompanying CFD advanced airbag simulations has been performed with Madymo 6.3.1 release [19]. The underlying numerical airbag model setup has been activated by the state-of-the-art capabilities of the Madymo integrated CFD Gasflow (GF) Module at the start of the presented study (please refer to [20], [21] and [22]). The effectiveness of the advanced airbag technology is investigated with the help of the advanced airbag CAE simulation methodology derived throughout the study and recorded also in [23], [24], [25].

The current paper documents the DAB module model setup and validation, and describes the findings applying the advanced simulation method to the OoP

occupant load case. Using the GF simulation method, the predicted dummy injury values are objectively compared to the ones observed in a real laboratory test. Questioning the quality of prediction, the potential of the CFD advanced airbag simulation method in terms of the development of new future technologies is discussed finally.

DAB MODEL

Analog to the main functional design parameters for finding an optimum solution for low-risk airbag deployment, the implementation of the most important physical properties of an OoP airbag model (inflator characteristics, cushion, folding, airbag door) are explained briefly within this chapter. The deployment characteristics of the advanced initially chambered DAB are discussed based on GF analysis and the model validation to dynamic pendulum deployment tests is explained in the final paragraph.

Inflator

The input to the airbag models is stated in terms of inflator exit gas temperature and mass flow rate. This input was generated using the MADYMO Tank test Analysis (MTA) programme which was used to convert experimental data for the ignition of the inflator in a closed tank to mass flow rate and temperature input (the empirical thermodynamic approach is explained in [26]). This data was validated by carrying out a 3-D tank test simulation (GF and uniform pressure (UP)) which was then compared to the experimental tank test records as shown in Figure 3. Please note that the pressure and time have been normalised to provide dimensionless units on the axis.

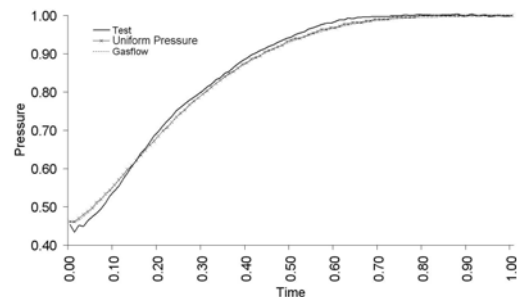


Figure 3. Tank pressure validation (GF and UP)

The above tank validation example shows the GF and UP pressure simulation time history versus the experimental pressure response of a single-stage

inflator output. Dual-stage output was applied for OoP application.

Cushion geometry and material

The fabric of the airbag was constructed using a FEM representation comprising the real geometry of the cushion. The whole airbag was split into two main chambers (2) and (3) during the modeling process (the additional chamber (1) was a dedicated chamber for the inflator). The inner chamber (2) represents the jet control in the early phase of deployment and the chamber (3) represents the remaining ring volume (please also refer to Figure 4 below).

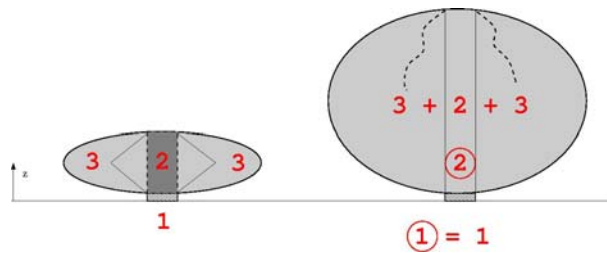


Figure 4. Initially chambered model before (left) and after (right) the rupture of the sacrificial tether

The initial two-chambered airbag evolves into a single-chambered airbag after the rupture of the sacrificial tether structure. Figure 5 shows the flat numerical model compared to the physical airbag.

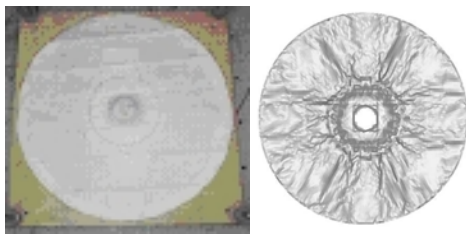


Figure 5. Physical flat airbag cushion (left) and the corresponding CAE model (right)

To cover the warp and weft fabric direction in the FEM model, the orthotropic fabric material model was implemented for the cushion as originally developed within [27]. Elastic fabric tensile material properties of the warp and weft direction were obtained from relevant tensile tests (possible test scenarios can be found in [28], [29]).

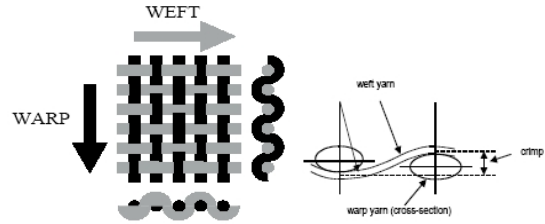


Figure 6. Warp and weft directions in woven fabric construction

Test matrix - The following material tests have been conducted (please refer to Table 1 below).

Table 1. Fabric material test matrix

Test	Static	Dynamic	Remarks
Tensile	X	X	Warp and weft
Bias	X	-	Picture frame

Bias tests were performed to identify the typical shear deformation mechanism that occurs in a plain-woven fabric as shown in Figure 7.

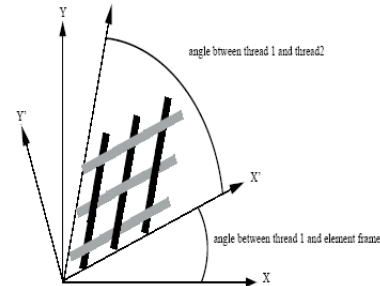


Figure 7. Shear deformation of woven fabrics [30]

The warp and weft yarns typically displace in a trellis-like manner under shear loading with little resistance until the yarn compaction or “lockup” angle has been reached which corresponds to an initial soft response of the fabric. The lockup angle is dependent on the yarn spacing and the geometry of the weave pattern.

Picture frame testing validation - To load the fabric specimen in shear direction, the following test setup with a picture frame was applied (see Figure 8).

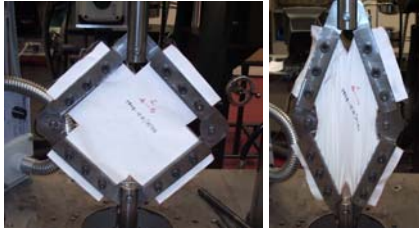


Figure 8. Picture frame test setup

The warp and weft thread properties incorporated from the tensile tests, together with the theoretically derived bias curve, lead to the following simulation of kinematics time history.

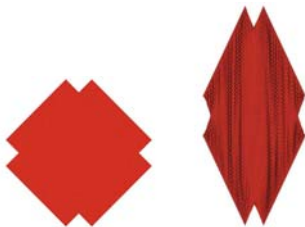


Figure 9. Picture frame simulation time history kinematics – non-deformed (left), deformed (right)

As observed in the test, the wrinkling of the fabric specimen also occurs in the simulated deformed frame. The diagram below shows the force-displacement response measured in the test versus the simulation time history curve.

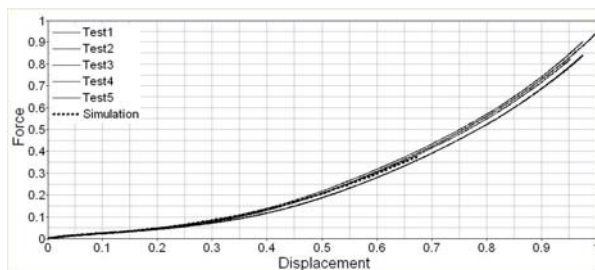


Figure 10. Picture frame force displacement

Although the MBS structure of the frame model was restricted to a determined shear movement, the simulation time history is closely validated to the test response.

Folding pattern

Folding is one of the most difficult tasks in an OoP simulation using CFD techniques. The flat 2-D cushion, which contains the main panels, internal chamber walls and conventional tethers leads to a stack of multiple fabric layers after folding. The

folded package cut view in Figure 11 gives an indication of the challenging folding task to be performed with the Madymo folder software [31].

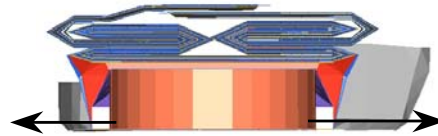


Figure 11. Folded cushion package cut view with inflator gas opening locations (arrows)

The inflator is modeled with multiple radial jets at the gas opening locations. The bag retainer (turning vane) also deflects gas and is therefore included in the simulation model. It is omitted only initially to implement the inflator jets in a vertical direction, as was previously examined in [32]. To cover the folded package dimensions of the real folded cushion fabric and to increase the surface ratio (initial mesh to reference mesh), a pre-simulation must be performed as described in the next paragraph. Handling folded FEM airbag cushions with the initial metric method (IMM) is further explained in [33].

Folded package pre-simulation - To implement the folded cushion into the bag holder, the dynamic relaxation shown in Figure 12 below is applied as a type of pre-simulation.

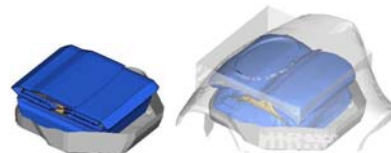


Figure 12. Cushion after folding (left) and the piston method mesh relaxation with boundary surfaces (right)

The dimensions of the folded package are restricted by a quadratic cube, the bag holder and the piston-like moving airbag door structure. The final relaxed mesh state of the pre-simulation leads to the folded cushion, which is finally implemented into the DAB module model.

Assembled DAB module - Figure 13 shows the folded cushion integrated in the bag holder and inflator model, as the assembled DAB module compared to the real hardware.

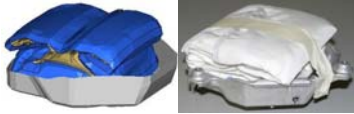


Figure 13. DAB model (left) and the hardware folded cushion package (right)

Airbag door

It is evident that the strength of the airbag door tear seam can have an impact on the punch-out phase of airbag deployment and therefore has a great influence on OoP load generation. Within the virtual state-of-the-art instrument panel development by structural FEM analysis, the airbag door characteristics also play a significant role. Therefore derivation of the elastic-plastic material properties is possible in accordance with the procedures described in [34]. Implicit structural FEM analysis (stress-strain analysis) as explained in [35] is also commonly applied within IP development. This approach was not applied within this study, but derivation of the material parameters with the help of physical tests helped to define practical experiments.

Test matrix - Table 2 provides an overview of the tests conducted.

Table 2. Airbag door material test matrix

Test	Static	Dynamic	Remarks
Tensile	X	X	Injected specimen
Tensile	X	X	Cut specimen
Impact	-	X	Full airbag door

The tensile test response of the injected specimen was used to implement the elastic-plastic properties. The test with the specimen cut from the airbag door identified the properties of the tear line. The airbag door-opening characteristic was then studied when a rigid impactor (simple airbag substitute) opened the tear line dynamically from the back.

Tensile testing validation - injected specimen - As an abstract of the tensile tests, Figure 14 through 16 below illustrate the injected plastic specimen and the static and dynamic test response versus the simulation force-displacement time history.

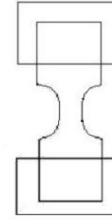


Figure 14. Injected plastic tensile specimen

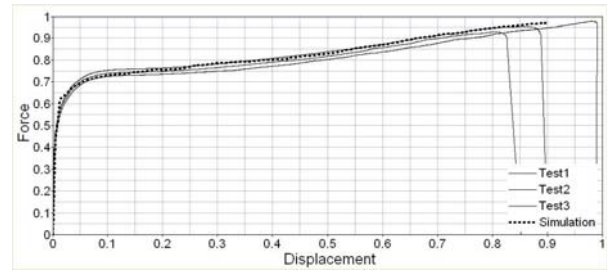


Figure 15. Static tensile force-displacement

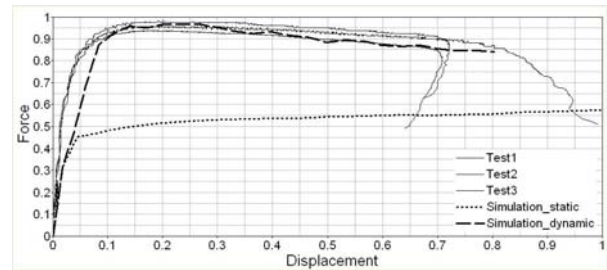


Figure 16. Dynamic tensile force-displacement

The derived plastic material model was then implemented into the full-size FEM model of the airbag door, which was validated in a dynamic impactor scenario as already mentioned above.

Full airbag door impactor testing validation - The dynamic test was conducted at high and low impactor velocities. In Figure 17, the simulation time history (left) and the test response (right) are shown for high velocity at 30 and 40 ms.

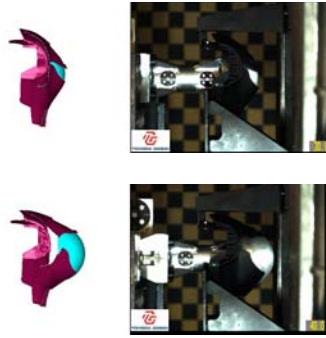


Figure 17. Airbag door-opening model at high impactor velocity; upper plot: at 30 ms; lower plot: at 40 ms

Door-opening kinematics are covered at both time points. To assess the accuracy of the simulation model, the impactor acceleration test response (during the opening process) was compared with the simulation acceleration time history (see Figure 18 below).

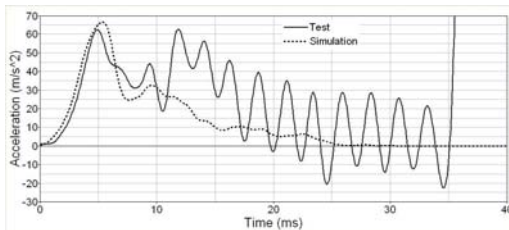


Figure 18. Impactor acceleration – at high velocity

The acceleration peak level at the moment of the tear line rupture – corresponding to the punch-out phase explained earlier – is also covered by the simulation. The further decrease in loading can also be seen, whereas friction between the impactor and the airbag door leads to some differences in test response and simulation time history.

The same scenario was also verified for a lower level impactor velocity. First the simulation time history (left), and then the test response (right), are pictured in Figure 19 at 60 and 70 ms.

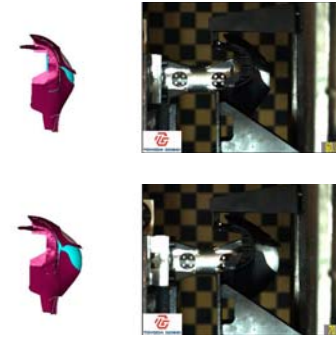


Figure 19. Airbag door-opening model at low impactor velocity; upper plot: at 60 ms; lower plot: at 70 ms

The tear line opening mode and acceleration peak for the lower impactor velocity are again reproduced by the simulation.

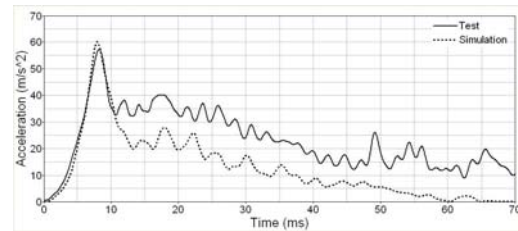


Figure 20. Impactor acceleration – at low velocity

Further, the acceleration peak level at the moment of the tear line rupture is covered by the simulation at the low impactor velocity. The further decrease in loading can be seen again, whereas friction between the impactor and the airbag door leads to some differences in test response and simulation time history.

DAB Simulation validation

Before discussing validation of the advanced DAB module in a simple physical pendulum environment, deployment of the flat airbag will be explained to analyse the real gas flow from the inflator to the initially chambered internal airbag volume. To dynamically validate the simulation model against a physical test, the airbag was made to hit a head form pendulum during the initial inflation (punch-out) phase. The acceleration test response was compared to the simulation time history obtained.

Gas flow control - To obtain an idea of the real gas flow within the chambered airbag volume, the non-folded flat airbag was statically deployed with single-stage inflator output.

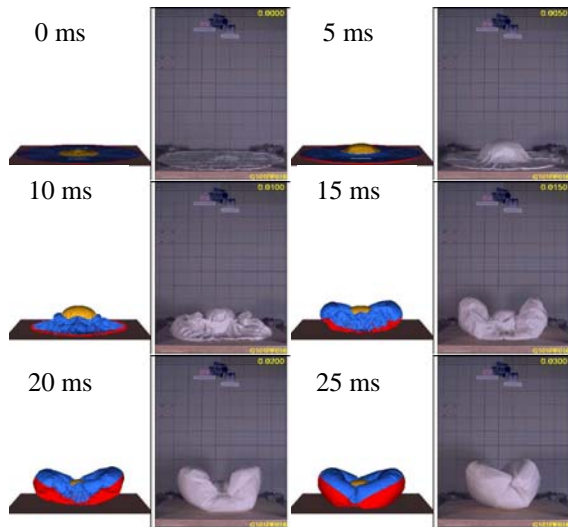


Figure 21. Deployment kinematics comparison for the first 25 ms of the real airbag and the simulation model

The inner tethers restrict the airbag's deployment throughout the 25 ms time. The accumulated internal pressure does not exceed the threshold to allow the sacrificial tether rupture. During the first 10 ms, hardly any gas is transported from the inner to the outer airbag chamber. Between 10 ms and 15 ms, the gas starts to move to the outer chamber, giving the deployed airbag a U-shape form, which is also effected by the outlet geometry between the airbag chambers.

A further academic comparison between the advanced airbag and a virtual conventional airbag (removed inner tethers) model was performed to analyse the gas jet path with the help of CFD result visualization. The calculated gas velocity vector plots are a good indication of the gas path as shown in Figure 22 below.

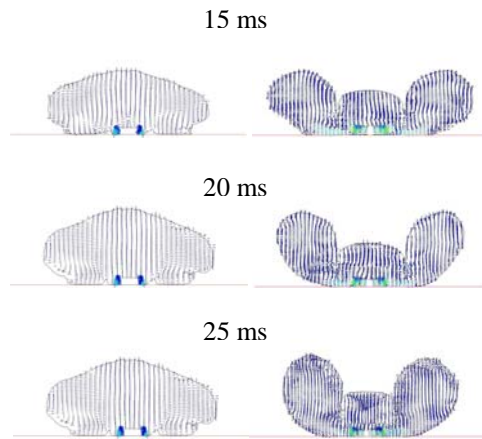
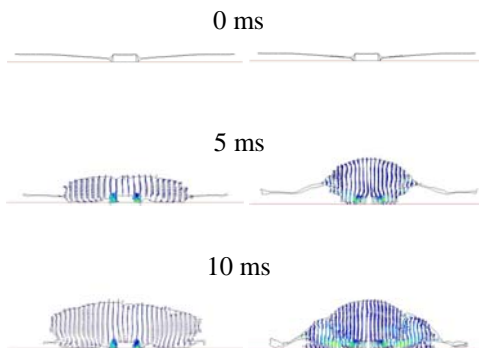


Figure 22. Comparison between the flat conventional (left) and flat advanced airbag (right) deployment kinematics in the first 25 milliseconds – CFD velocity vector plots

During the first 15 ms –indicated here as the punch-out phase - the vector plot clearly illustrates the difference between both airbag designs. Whereas the airbag's inner chamber is filled first and the inflator gas starts to flow to the outer tether at approx. 10 ms, the gas flow is not re-directed in the conventional cushion. If 15 ms to 25 ms could be indicated as the membrane-loading phase, the above plot shows the significant difference of the airbag expansion distance at the centre of both bags.

A brief analysis of the academic example suggests the GF CFD airbag simulation potential to provide detailed evaluation of the real gas flow within, here the chambered airbag volume. This advanced simulation method constitutes a powerful tool to evaluate, features such as orifice geometry and location to further optimise the low risk airbag deployment functionality.

DAB model validation - Dynamic head form pendulum tests were performed to validate the DAB module model with the equipped airbag door. At a defined close distance, the airbag hits the head form during the initial deployment phase. Figure 23 shows the simulation animation (left) versus the test (right).

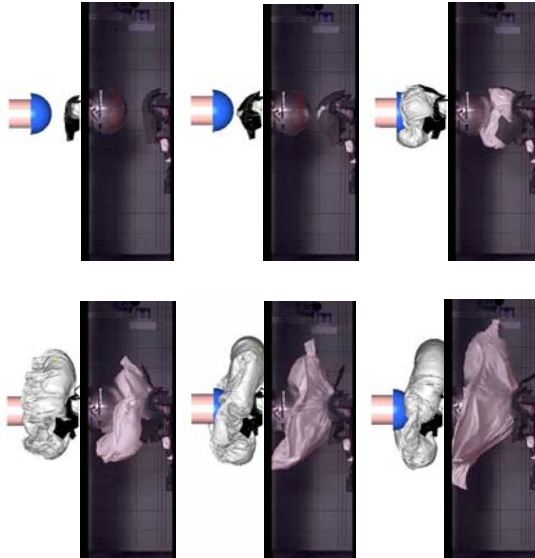


Figure 23. Head form simulation (left) versus test (right) – initial deployment – 0ms to 10 ms in 2ms steps

The simulation supplies a realistic airbag door-opening mode together with reasonable cushion deployment kinematics. The pendulum acceleration time history and the test response are compared in the following diagram (Figure 24).

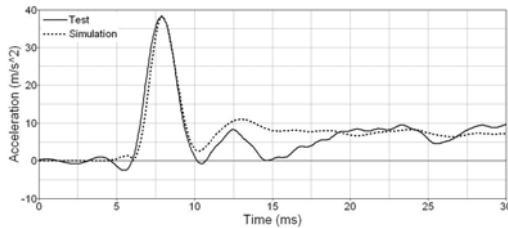


Figure 24. Head form acceleration test response versus simulation time history

The punch-out acceleration peak is covered by the simulation model. The validated DAB module model was applied in the OoP occupant simulation as discussed in the next paragraph. The resulting dummy injury values are expected to provide an indication of the airbag membrane-loading phase explained above.

OOP OCCUPANT TEST

To verify protection in an OoP situation, three different options can be considered in development according to FMVSS 208, whereby the major OoP

option applied by automobile manufacturers is the so-called “low risk deployment”. In the following Table 3, which contains the FMVSS 208 OoP injury value limits, this is referred to as “static”.

Table 3. FMVSS 208 OoP injury value limits

AF05 injury criteria limits		Crash	Static
Head	HIC15 [-]	700	700
Neck	Nij [-]	1.0	1.0
	Tension [N]	4287	3880
	Compression [N]	3880	3880
	Flexion [Nm]	155	155
	Extension [Nm]	67	67
	Max tens. [N]	2620	2070
	Max comp. [N]	2520	2520
Chest	Accel. 3 ms [g]	60	60
	Deflection [mm]	52	52
Femur	Force [N]	6.8	6.8

The static option is verified with static deployment tests where the dummy is positioned close to the airbag module. The OoP test scenario was set up within this study in a generic laboratory environment according to the FMVSS 208-regulated AF05 female dummy positions:

- Position 1: Chin on module
- Position 2: Chin on rim

The following Figure 25 and 26 show the OoP occupant test setup for both positions:



Figure 25. Position 1 – side and front view of test setup

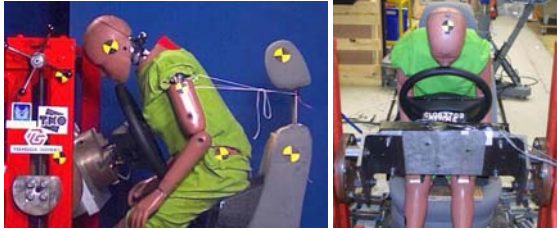


Figure 26. Position 2 – side and front view of test setup

In real vehicle environments, the windshield sometimes affects the dummy position 2. Correcting the steering-wheel angle is therefore a permissible procedure in order to avoid contact between the dummy head and the windshield. In the laboratory test, the steering-wheel angle could be kept constant for both dummy postures. To reproduce the exact dummy position later in the simulation approach, dummy target points were determined using a 3-D measurement device.

OCCUPANT OOP SIMULATION

The validated DAB module, including the airbag door, was inserted into the detailed steering-wheel model as indicated in Figure 27.

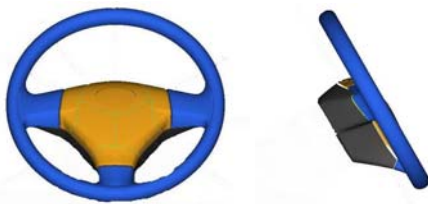


Figure 27. Detailed FEM steering-wheel model – front view and side view

The rim and the back cover were implemented as non-deformable rigid contact surfaces. The following Figures 28 and 29 depict the OoP occupant models for both positions.

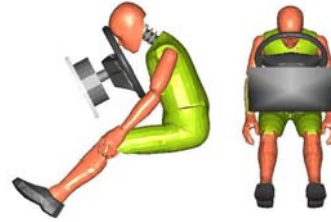


Figure 28. Position 1 – simulation model side and front view

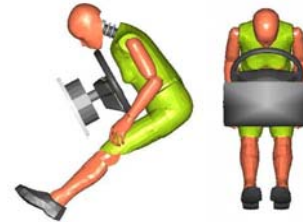


Figure 29. Position 2 – simulation model side and front view

Madymo's AF05 facet data base dummy posture corresponds to the 3-D target points reported during testing.

Occupant position 1 results

Figure 30 shows the initial airbag deployment kinematics (simulation: left; test: right) at 10, 20 and 30 ms from the side view.

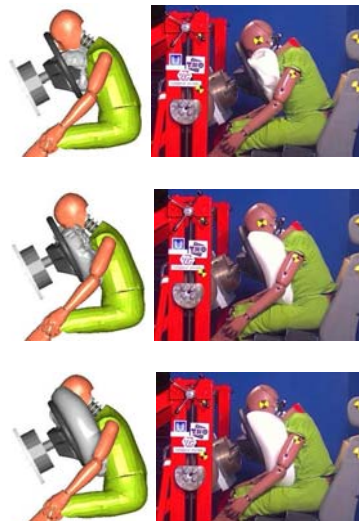


Figure 30. NHTSA position 1, test (right) versus simulation (left) for 10, 20 and 30 ms – side view

In simulation, friction between the airbag and the dummy influences airbag deployment towards the femurs and therefore a slight difference in kinematics

occurs in comparison to the test response. Table 4 lists the injury peak values reached in the test versus the simulation time history.

Table 4. Test and simulation OoP injury values – OoP position 1

AF05 injury criteria OoP position 1		Test average	Simulation
Head	HIC15 [-]	26	11
Neck	Nij [-]	0.24	0.24
	Tension [N]	580	890
	Compression [N]	20	70
	Flexion [Nm]	18	22
	Extension [Nm]	5	1
Chest	Accel. 3 ms [g]	11.0	8.2
	Deflection [mm]	9	7

Because the femur forces play a minor role within the laboratory test (no contact to an instrument panel was possible), they are not discussed further here. Whereas the neck values are overestimated by simulation, the simulated chest values are slightly lower than the test response. To evaluate the punch-out and the membrane-loading phases and their dummy injury cause in more detail, a closer look is taken at the injury curve characteristics below. As for dummy position 1, in which the chin is positioned closely in front of the airbag module, the punch-out phase greatly influences the head and neck dummy body area. Figures 31 to 33 plot the head and neck injuries obtained by the simulation model versus the test response for dummy position 1.

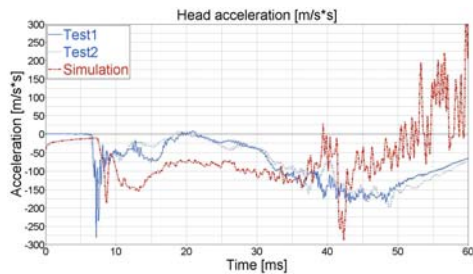


Figure 31. NHTSA position 1, injuries test versus simulation – head X-acceleration

The initial peak can not be correctly covered by the simulation for head acceleration, but is well reproduced for the upper neck force (punch-out effect).

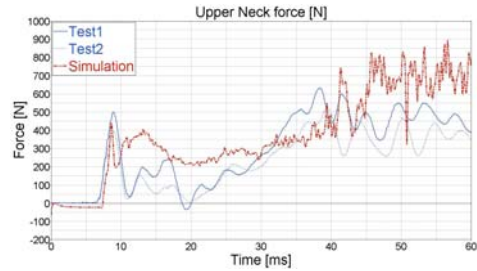


Figure 32. NHTSA position 1, injuries test versus simulation – upper neck Z-force

The membrane-loading phase (here approx. 10 ms to 40 ms) can be seen in the simulation. The released energy is relatively well transferred to the dummy in the simulation.

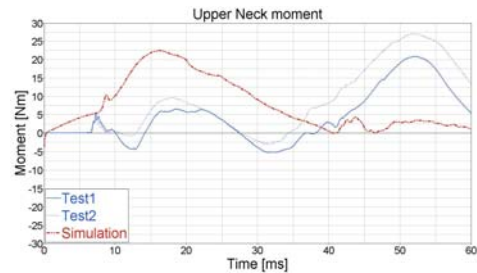


Figure 33. NHTSA position 1, injuries test versus simulation – upper neck Y-moment

Overestimating the neck moment timing, the injury value tendency of the head and neck can be predicted by the GF simulation. Figure 34 indicates the dummy test response versus the simulation time history of the dummy chest acceleration and chest deflection.

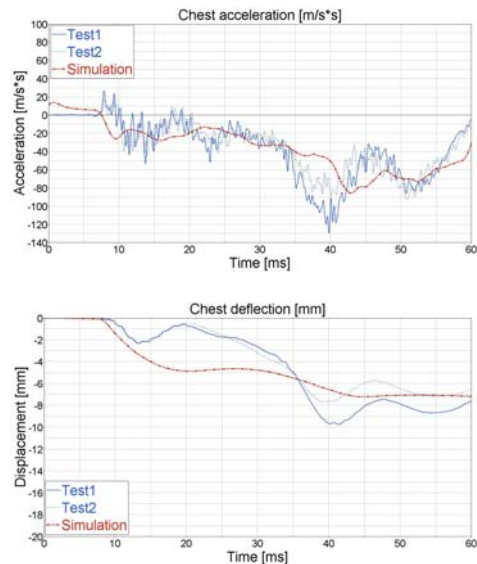


Figure 34. NHTSA position 1, injuries test versus simulation – chest X-acceleration and deflection

With respect to the dummy's measurement tolerance, the chest injury values are predicted by the GF simulation. The curve characteristics of the test response for the chest mark the membrane-loading phase (load increase to 40 ms). A good trend can be obtained by the advanced simulation method.

Occupant position 2 results

Figure 35 indicates the initial airbag deployment kinematics (simulation left versus test right) at 10, 20 and 30 ms from a side view for dummy position 2.

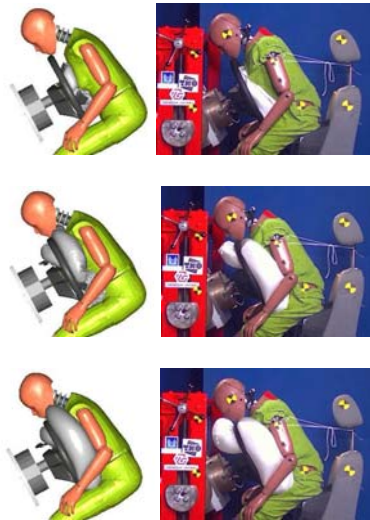


Figure 35. NHTSA position 2, test (right) versus simulation (left) for 10, 20 and 30 ms – side view

In simulation, the airbag mainly deploys below the upper rim of the steering-wheel. The friction between the airbag and the dummy could cause the differences compared to the test. Before the curve characteristics of the injury values are discussed in brief, Table 5 below lists the injury peak values – test versus simulation.

Table 5. Test and simulation OoP injury values – OoP position 2

AF05 injury criteria OoP position 2		Test average	Simulation
Head	HIC15 [-]	7	8
Neck	Nij [-]	0.18	0.33
	Tension [N]	430	570
	Compression [N]	25	30
	Flexion [Nm]	5	7
	Extension [Nm]	10	20
Chest	Accel. 3 ms [g]	11.7	10.7
	Deflection [mm]	20	23

The simulation slightly overestimates all the injury values. Figure 36 to Figure 38 plot the dummy head and neck injuries obtained by simulation versus the test response for dummy position 2.

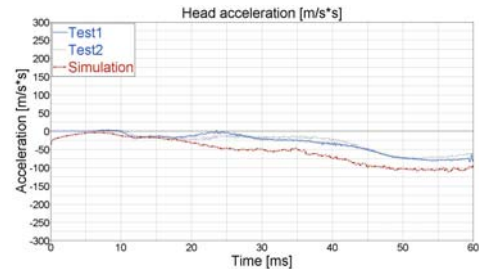


Figure 36. NHTSA position 2, injuries test versus simulation – head X-acceleration

The curve characteristic is followed well by the simulation.

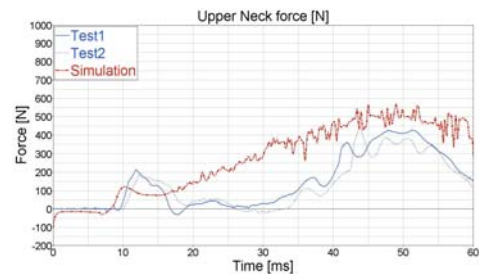


Figure 37. NHTSA position 2, injuries test versus simulation – upper neck Z-force

As already mentioned above, simulation overestimates the upper neck force. The increase of force during full deployment (membrane-loading phase) is covered by tendency.

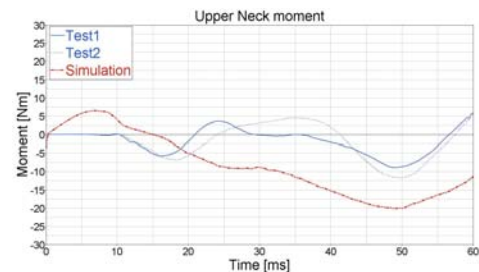


Figure 38. NHTSA position 2, injuries test versus simulation – upper neck Y-moment

The head acceleration and the neck force can be predicted by simulation, whereas differences within the neck moment are obtained. Figure 39 indicates

the dummy chest simulation time history versus the test response.

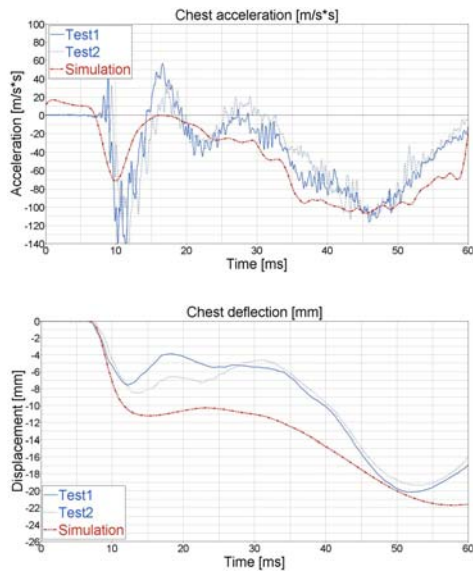


Figure 39. NHTSA position 2, injuries test versus simulation – chest X-accelerations and deflection

For position 2 (chest on module), the airbag punch-out effect affects the dummy chest body area more, whereas the head and neck injury values provide an indication of the membrane-loading phase. The punch-out phase in chest acceleration is covered by tendency but can not match the test response peak value. The load transfer during full airbag deployment (membrane-loading) is reproduced well by the advanced simulation.

DISCUSSION

Identification of the essential parameters by means of the appropriate experiments and CAE methods to model the folded airbag module leads to reasonable airbag validation within the simple one degree of freedom pendulum scenario (punch-out effect). Further replacement of the pendulum by the dummy model with its sophisticated contact surfaces such as head, neck, chest, arms and shoulders increases the numerical complexity. The thermodynamic energy released by the chambered airbag module presented is transferred to the dummy via the CFD gas transport algorithm (fluid-structure interaction) and finally by means of the numerical contact mechanics between the cushion and the dummy surfaces during the early stage of airbag deployment. The different loads measured in the dummy indicate the energy transmission in more detail. The airbag punch-out

and membrane-loading phase tendency observed in the laboratory tests are covered by the OoP simulation as a result of the investigation of the low-risk effectiveness of the initially chambered DAB design. Generally speaking, the FMVSS 208 relevant dummy load levels can be predicted by the advanced GF airbag simulation method using Madymo's facet data base dummy model. Whereas the CFD results are close to experimental response, there are still some differences, e.g. in the dummy neck injuries as also reported in [36] and in deployment kinematics, which need to be analysed further. With the application of the FEM AF05 dummy designed for the OoP load case, a further improvement in result quality is expected. The FEM dummy is equipped with more detailed upper body description (head, neck and chest contact surfaces) and improved soft tissue compliances (material model).

In the automotive industry's product development process, analysis and physical prototyping have co-existed for years. Being the key to a higher level of competitiveness in terms of faster-to-market and cost reduction for OEMs and suppliers, a big push in the direction of 100% virtual prototyping is going to take place in the near future in the area of CAx data management and processes as presented in [37] and [38]. What does this and the above summarised results of the OoP simulation with the advanced chambered airbag mean for the future development and design of new airbag technologies?

Based on the current study experience, it is the author's opinion that 100% virtual airbag prototyping and validation will be difficult to reach in the near future, not only because of the challenges in simulating long-term durability or aging, but also due to the following major hurdles in design disciplines which need to be overcome:

1. Inflator characteristics applied in the study are based on over-simplified assumptions (MTA). Intensive research work and collaboration with inflator suppliers is still required to identify correct inflator gas initial conditions and characteristics for CFD integrated airbag models.
2. Although the folder software and contact algorithm can handle the presented complex 2-D DAB cushion from folding over folded mesh relaxation, it is still a time-consuming process within the industrial design procedure. Further folding process optimisations are necessary which also take into consideration the complex folding of 3-D passenger airbags with internal gas deflection to improve the effective

application of the presented advanced airbag simulation methodology.

3. The accuracy and robustness of constitutive material models for engineering plastics and polymeric foams under high strain rate and large deformations for airbag door modelling as well as for robust response of local airbag dummy interactions (improvement of dummy model robustness).
4. In order to investigate the effects of design parameter variations, a vast amount of computing resources are needed.

CONCLUSION

The presented advanced initially chambered driver airbag performs in reality and virtually far below the injury value limits required by FMVSS 208. The advanced CFD airbag simulation methodology allows a deep insight into better understanding the physical problems. Therefore it is a helpful and powerful tool for pushing the future development of new airbag technologies. For instance by changing the cushion geometry – here the inner control volume of the presented chambered airbag – the effect on risk performance can be studied with numerical simulation. In mathematical terms, an approximation of the inner control volume size to the airbag volume itself leads to a conventional airbag. But shrinking with parallel application of new materials (to avoid burning) could lead to the next generation of advanced airbags designed for the low risk deployment target. Further, the CFD integrated simulation allows investigation into the effectiveness of different folding patterns in order to evaluate the consequences for the gas jet path and for the ensuing dummy injury values. The challenge of solving the airbag risk and protection compromise tells its own tale that further investment into the advanced airbag simulation methodology, as presented in this paper, will be a technically profitable task for the future.

REFERENCES

1. *Driver fatalities in 1985-1994 air bag cars.* Ferguson S.A., Lund A.K., Greene M.A., Insurance Institute for Highway Safety, Arlington, USA, 1995.
2. *Risk of death among child passengers in front and rear seating positions.* Braver E.R., Whitfield R.A., Fergusson S.A., Child Occupant Protection 2nd Symposium Proceedings (P-316), SAE, pp 25-34.
3. *Crash investigation reports.* U.S. NHTSA Department of Transportation, Washington DC, USA, 1998.
4. *5th Percentile Driver Out of Position Computer simulation.* R. Roychoudhury, D. Sun, M. Hamid, C. Hanson, SAE Paper 2000-01-1006.
5. *Driver Fatalities in Frontal Crashes of Airbag Equipped Vehicles: A Review of 1989-1996 NASS Cases, Accident Research and Analysis.* Cammisa X.C., Ferguson S.A., Lund A.K., SAE Paper 2000-01-1003.
6. *Assessment of Airbag Deployment Loads.* Horsch J., Lau I., Miller G., SAE Paper 902324.
7. *Dual-Stage Inflators and OoP Occupants - A Performance Study.* Malczyk A., Franke D., Adomeit H.-P., SAE Paper 982325.
8. *Ringairbag – Smart Driver Airbag Concept.* Krönes W., Schmidt W., 6th International Symposium and Exhibition on Sophisticated Car Occupant Safety Systems, Karlsruhe Germany, December 2002.
9. *Influence of Air Bag Folding Pattern on OOP-injury Potential.* Mao Y., Appel H., SAE Paper 2001-01-0164.
10. *A Math-Based CAE High-Speed Punch Methodology for Polymer Airbag Cover Design.* Lee M.C., Novak G.E., SAE Paper 2006-01-1187.
11. *Out of Position Simulation – Possibilities and Limitations with Conventional Methods.* Beesten B., Hagen S., Rabe M., 6th International Symposium and Exhibition on Sophisticated Car Occupant Safety Systems, Karlsruhe Germany, December 2002.
12. *Development of a Benchmark Problem Set for Assessing Out-of-Position Simulation Capabilities.* Wenyu Lian, SAE Paper 2004-01-1628.
13. *Numerical Simulation of Fully Folded Airbags and Their Interaction with Occupants with Pam-Safe.* Lasry D., Hoffmann R., Protard J.-B., SAE Paper 910150.

14. *Airbag modelling for Out-of-Position: Numerical approach and advanced airbag testing*. Rekveldt M., Swartjes F., Steenbrink S., Madymo User Conference, Como, Italy, October 2002.
15. *Advanced Airbag Fluid Structure Coupled Simulations Applied to Out-of-Position Simulations*. Ullrich P., Tramecon A., Kuhnert J., ESI Distributions, 2000.
16. *Simulation of Airbag Deployment Using a Coupled Fluid-Structure Approach*. Souli M., Olovsson L., Do I., 7th International LS-DYNA Users Conference, 2002.
17. *Evaluation and Comparison of CFD Integrated Airbag Models in LS-DYNA, MADYMO and PAM-CRASH*. Zhang H., Raman S., Gopal M. Han T., SAE Paper 2004-01-1627.
18. *OOP-Simulation – A Tool to Design Airbags? Current Capabilities in Numerical Simulation*. Beesten B., Hirth A., Reilink R., Remensperger R., Rieger D., Seer G., 7th International Symposium and Exhibition on Sophisticated Car Occupant Safety Systems, Karlsruhe Germany, November 2004.
19. *Madymo 6.3.1 Reference / Theory Manual*. TNO Madymo BV. Delft, The Netherlands. August 2006.
20. *Fully Multidimensional Flux-Corrected Transport Algorithms for Fluids*. Zalesak S.T., Journal of Computational Physics Vol. 31, pp 335-362, 1979.
21. *Solution of Continuity Equations by the Method of Flux-Corrected Transport*. Boris J.P., Book D.L., Methods in Computational Physics Vol. 16, Academic Press, 1976.
22. *Numerical Modelling of the Inflation Procedure of an Airbag and the Thermo-Chemical Process in the Gas Generator*. Rieger Doris, Institute of Aeronautics, Technical University Munich, October 2005.
23. *A Simulation Approach for the Early Phase of a Driver Airbag Deployment to Investigate OoP Scenarios*. Mahangare M., Trepess D., Blundell M.V., Freisinger M., Hoffmann J., Smith S., European Madymo User Conference, Cambridge, UK, September 2005.
24. *A Methodology for the Simulation of Out-of-Position Driver Airbag Deployment*. Mahangare M., Trepess D., Blundell M., Freisinger M., Hoffmann J., Smith S., International Journal of Crashworthiness, pp 511-517, November 2006.
25. *Investigation of an Advanced Driver Airbag Out-of-Position (OoP) Injury Prediction with Madymo Gasflow Simulations*. Freisinger M., Hoffmann J., Blundell M., Mahangare M., Smith S., International Madymo User Conference, Detroit, USA, November 2006.
26. *Advances in Airbag Inflator Modelling*. Bosio A.C., Lupker H.A., 4th International MADYMO Users Meeting, Eindhoven, The Netherlands, 1993.
27. *The Development and Validation of the Material Model Fabric_Shear for Modelling Advanced Woven Fabrics*. U. Stein, G. Weissenbach, M. Schlenger, M. Tyler-Street, P. Ritmeijer. 10th International Users Meeting. Amsterdam, The Netherlands. October 2004.
28. *A Study on the Modelling Technique of Airbag Cushion Fabric*. Hong S., Park S., Kim C., 9th International MADYMO Users Meeting, 2002.
29. *An Integrated Testing and CAE Application Methodology for Curtain Airbag Development*. Narayanasamy N., Hamid M., Ma D., Suarez V., SAE Paper 2005-01-0289.
30. *Airbag Fabric Picture Frame Test Manual. Version 1.0*, TNO MADYMO BV, 2005.
31. *Madymo Folder - Folding Airbag Models Version 9.0*. Oasys Limited. London, UK. November 2003.
32. *Capability of Simplified Folded Airbag Models in Gasflow Simulations*. Doris Rieger. 4th European Madymo User Conference. Brussels, Belgium. October 2004.
33. *Airbag Modelling Using Initial Metric Methodology*. Tanavde A., Khandelwal H., Lasry D., Ni X., Haug E., Schlosser J., Balakrishnan P., SAE Paper 950875.
34. *Analytical Design of Cockpit Modules for Safety and Comfort*. Lin J.Z., Pitrof S.M., SAE Paper 2004-02-1481.
35. *Validation/Verification of Hidden Airbag Door Loads and Kinematics*. Coulton J., CAD-FEM Users Meeting – International Congress on FEM Technology, Friedrichshafen, Germany, 2002.
36. *Use of MADYMO CFD for Driver Out of Position Simulation*. Lee W., SAE Paper 2006-01-0825.
37. *Digital Prototypes: Another Milestone for the Improvement of Processes and Cooperation in Vehicle Development*. Breitling T., Dragon L., Grossmann T., International VDI Symposium of Numerical Analysis and Simulation in Vehicle Engineering, Würzburg, Germany, 2006.
38. *Data Management, Process Support and CAx Integration of Engineering at Audi*. Reicheneder J., Gruber K., Wirch, W., Mayer S., International VDI Symposium of Numerical Analysis and Simulation in Vehicle Engineering, Würzburg, Germany, 2006.